Using CALIOP to estimate the base height of optically thick clouds
Used to be: "Optimized Detection by Radar/lidAr for base of Nuages (ODR/AN)"

Johannes Mülmenstädt[1], Odran Sourdeval[1], Christoph Böhm[2], and Johannes Quaas[1]

[1]Institute of Meteorology, Universität Leipzig, Leipzig, Germany
[2]Institute of Meteorology, Universität Köln, Köln, Germany

Correspondence to: Johannes Mülmenstädt (johannes.muelmenstaedt@uni-leipzig.de)

Abstract. A measurement technique is presented that uses CALIOP lidar profiles to estimate cloud base heights. The technique provides cloud base heights even when clouds are thick enough to attenuate the lidar beam (optical thickness $\tau \gtrsim 5$) by treating the cloud base height of nearby thinner clouds as representative of the entire cloud field. Using ground-based ceilometer data, uncertainty estimates are derived as a function of various properties of the CALIOP lidar profiles. Evaluation of the predicted cloud base heights and their predicted uncertainty using a second, statistically independent, ceilometer data set shows that cloud base heights and uncertainties are biased by less than 10%.

1 Introduction

Cloud base height is an important geometric parameter of a cloud. It controls how much downwelling longwave radiation the cloud emits. Aerosol concentration and updraft speed at that level control the microphysics of the cloud. It is one of the parameters that is required in the calculation of the subadiabaticity of the cloud. However, due to the viewing geometry, it is also one of the most difficult parameters to retrieve from satellite.

Multiple methods have been proposed for satellite determination of the cloud base height. VIIRS cloud-base temperature method: Zhu et al. (2014, doi 10.1002/2013GL058970). Results of evaluating cloud base heights inferred from oxygen absorption bands and from MISR stereoscopic images will be reported in separate manuscripts. For analyses wishing to combine cloud base information with other cloud properties retrieved by A-Train satellites, these methods share the disadvantage that the required instruments are not part of the A-Train. Methods that are applicable to A-Train satellites are based on MODIS cloud properties retrieved near cloud top and integrated along moist adiabats to determine the cloud thickness (Meerkötter and Zinner (2007) (10.1029/2007GL030347)) or on

active remote sensing by CloudSat (2B-GEOPROF, Marchand et al) or a combination of CloudSat and CALIOP (2B-GEOPROF-LIDAR, Mace and Zhang 2014). The MODIS-derived cloud thickness assumes adiabatic cloud profiles and therefore cannot be used to constrain subadiabaticity. CloudSat misses the small droplets at the base of nonprecipitating clouds, and retrievals are further degraded in the ground clutter region. CALIOP detects the bases of only the thinnest clouds ($\tau < 5$, according to Mace and Zhang, 10.1002/2013JD021374); frequently, it is desirable to know the base height of thick clouds as well.

In this paper, we revisit the CALIOP cloud base determination. Because the lifting condensation level is approximately homogeneous within an airmass, the cloud bases retried by CALIOP for thin clouds may be a good proxy for the cloud base heights of an entire cloud field, including the optically thicker clouds within the filed. We have designed an algorithm that extrapolates the CALIOP cloud-base measurements into locations where CALIOP attenuates before reaching cloud base. This algorithm is called CBASE (Cloud Base Altitude Spatial Extrapolator). In this paper we evaluate its performance by comparing CBASE cloud base heights against cloud base heights observed by ground-based ceilometers.

Section 2 describes the data sources used in determining and evaluating the cloud base height. In Section 3 we describe the algorithm and evaluate its performance, including error statistics. The processed CBASE output available at DKRZ is described in Section 4. We conclude in Section 5 with an outlook on the longstanding questions that the CBASE data set can address.

2   Data

Two classes of data are used in this work. The first class satellite data, which we use with the intent of deriving a global data set of cloud base height. The second class is ground-based observations of "true" cloud base height used to tune and evaluate the algorithm by which cloud base height is determined from the satellite data.

2.1   CALIOP VFM

The input satellite data to our analysis is the CALIOP vertical feature mask (VFM). For each CALIOP lidar backscatter profile, the VFM identifies features such as clear air, cloud, aerosol, or surface; this is termed the "feature type". In addition to the feature type, the VFM records the degree of confidence in the identification ("none" to "high", termed the "feature type QA flag"); the thermodynamic phase of a layer identified as cloud as well as the degree of confidence therein (termed "ice water phase" and "ice water phase QA flag"); the horizontal distance over which the algorithm had to average to identify a feature above noise and molecular atmospheric scattering ("horizontal averaging distance").

2

In the present analysis, we use VFM version 4.10 (**?**), the current "standard" release. The VFM files are obtained from ICARE.

2.2 Airport ceilometers

For optimizing several tunable parameters of the algorithm, and for evaluation of the tuned algorithm, "true" cloud base heights need to be known. The source of these "true" cloud base heights in this work are ground-based cloud observations in aviation routine and special weather reports (METARs and SPECIs, collectively referred to as METARs henceforth; `https://library.wmo.int/pmb_ged/wmo_49-v` In METARs, cloud base heights are measured by ceilometer over a period of time (tens of minutes) and objectively grouped into cloud layers and their respective fractional coverages, using the temporal variation at a fixed point under an advected cloud field as a proxy for spatial variability of the cloud field.

To ensure that the ceilometer cloud base heights are of high and spatially uniform quality, we restrict ourselves to METARs from the contiguous continental United States, where the cloud base height is mostly derived automatically by laser ceilometers that form part of Automated Surface Observing Stations (ASOS, `http://www.nws.noaa.gov/asos/pdfs/aum-toc.pdf`) system. In other parts of the world, the cloud bases may be estimated by human observers or may be omitted under certain conditions when the lowest cloud base is higher than 5000 feet.

To obtain an unbiased estimate of the algorithm performance, it is necessary to use an evaluation data set that is statistically independent of the tuning data set. We use METARs from the year 2008 for tuning. Once the tuning is complete, we then use METARs from the year 2007 for evaluation.

{ j_μ: The ASOS data is used, among other purposes, for assimilation in NWP (HRRR and IFS citation). In METAR format, it is distributed globally by the WMO and widely archived. The data for the present analysis was downloaded from the Weather Underground (citation?). }

3   CBASE Algorithm and evaluation

The CBASE algorithm and evaluation proceed in four steps:

1. We determine the cloud base height from all CALIOP profiles where the surface generates a return ($\longrightarrow$ lidar is not attenuated above cloud base). We refer to these cloud base heights as *local cloud base heights* in the sense that they are local to the CALIOP profile.

2. Using ground-based ceilometer data, we determine quality of cloud base height depending on a number of factors. { j_μ: Refer to this as "tuning", and define it in the context of supervised machine learning.}

3

3. Based on the predicted quality of each local cloud base, we either reject the local cloud base or combine it with other local cloud bases within a distance $D_{\max}$ of the point of interest (POI) $\longrightarrow$ estimate of cloud base height, estimate of cloud base height uncertainty

90   4. Using a statistically independent validation dataset, we verify that the predicted cloud base height and uncertainty are correct.

At several points in the algorithm development, it is necessary to know the true (ceilometer-observerd) cloud base height. We use ceilometer observations from the year 2008 at those points. A statistically independent data set is required for an unbiased evaluation of the algorithm performance;

95   we use the year 2007. {j_μ: Not sure whether this paragraph is better placed here or in the previous section.}

This section is divided into four subsections, one for each algorithm step enumerated above.

Figure 1 illustrates the method.

3.1   Determination of local cloud base height

100   Source of local cloud base from the CALIOP VFM: any profile with a surface return.

3.2   Determination of local cloud base quality

We assess the quality of the CALIOP cloud base height z using the ceilometer-observed cloud base height $\hat{z}$ using root mean square error (RMSE), defined as

$$E = \sqrt{\frac{1}{N} \sum_{i=1}^{N} (z_i - \hat{z})^2}. \tag{1}$$

105   The sum runs over all CALIOP profiles containing a cloud layer and a surface return that are within 100 km horizontal distance of the ceilometer, occurred within 3600 s of a ceilometer observation, and have their lowest CALIOP cloud feature within 3 km of the surface. Ceilometer observations are only used if the observation closest in time to the Calipso overpass contains a cloud within 3 km of the surface. A height limit is imposed because a subset of the ceilometers has a range limit of

110   12500 feet, and all ceilometers report ceilings above 10000 feet with reduced granularity (500 feet); the 3 km threshold avoids those ceilometer limitations and mimics the ISCCP definition of low cloud ($p > 690$ hPa).

The following metrics, which are useful for a qualitative assessment of the quality of the satellite cloud base, are also calculated, but play no quantitative role in the algorithm:

115   **Correlation coefficient** between the CALIOP cloud base and ground-based observation of the cloud base. We use the Pearson correlation coefficient. Ideally the correlation coefficient would be unity.

Linear regression slope and intercept (ideally 1 and 0, respectively).

Retrieval bias, defined as

$$\text{bias} = \frac{1}{N}\sum_{i=1}^{N}(z_i - \hat{z}),\tag{2}$$

(ideally 0)

Efficiency, i.e., probability that a retrieval is available at the desired location (ideally 1).

CALIOP's ability to detect cloud base depends on the properties of the cloud. Therefore, we expect that the cloud base height quality will vary between different cloud profiles. Measuring the quality as a function of various properties of the CALIOP column may allow us to predict the quality of other columns with the same combination of properties. The properties that are easily accessible in a single column and have the greatest effect on quality are:

- horizontal distance D from the ceilometer,

- number of column cloud bases within horizontal distance D_{max},

- CALIOP VFM feature quality assurance flag,

- geometric thickness of the lowest cloud layer,

- CALIOP thermodynamic phase determination of lowest cloud,

- feature type, if any, detected between the lowest cloud and the surface,

- and horizontal averaging distance required for CALIOP cloud feature detection.

For illustrative purposes, Figure 2 shows the joint distribution of CALIOP and ceilometer cloud base height faceted by the CALIOP VFM feature quality assurance flag.

Based on determining the retrieval quality one variable at a time, the following classes of CALIOP profiles are discarded:

- CALIOP VFM quality assurance worse than "high" ,

- "invalid" or "no signal" layers between the surface and the lowest cloud layer (indicating that although the surface may generate a detectable return, the lidar is sufficiently attenuated that the cloud base, which scatters less strongly than the surface, is unreliable),

- minimum CALIOP cloud detection horizontal averaging distance within the lowest cloud layer greater than 1 km,

- or phase of the lowest layer determined to be other than liquid by the CALIOP VFM algorithm (the reason for this is that not enough such columns exist to determine the RMSE reliably in each of the categories defined below).

5

The remaining variables are discretized roughly into quintiles with the following boundaries:

- horizontal distance D from the ceilometer, with boundaries 0, 40, 60, 75, 88, and 100 km (distance greater than 100 km is discarded),

- number of CALIOP columns n with a cloud layer and a surface return within 100 km horizontal distance from the ceilometer, with boundaries at 0, 175, 250, 325, 400 (multiplicities greater than 400 are accepted),

- geometric thickness Δz of the lowest cloud layer, with boundaries at 0, 0.25, 0.45, 0.625, and 1 km (thickness greater than 1 km is accepted).

We can now consider the joint distribution of CALIOP and ceilometer cloud bases for each combination of the above variables. (Base heights above ground are used to remove an intrinsic correlation due to terrain.) Because of the viewing geometry, high CALIOP cloud bases tend to be overestimates where a higher layer obscures a lower layer. { j_μ: Isn't the actual reason a combination of regression dilution at the extremes of the distribution and phase space truncation at a physical boundary for low cloud bases?} It is desirable to correct for this bias. The options are no correction, a linear correction (which partially corrects for the high bias of high CALIOP base heights but introduces a counterbias at low CALIOP base heights), and a nonlinear correction that does not suffer from the counterbias at low CALIOP base heights. Our choice for nonlinear correction is a support vector machine. The final choice of correction is based on the performance of the three options on the tuning sample after combination has been performed according to the next step of the algorithm (Section 3.3).

Following bias correction, the sample RMSE is calculated for each combination of D, n, and Δz. The sample RMSE is taken as an estimate of the statistical uncertainty $\sigma(D, n, \Delta z)$ on the CALIOP cloud base height.

3.3 Combination of local cloud bases

CALIOP cloud base heights only exist sporadically { j_μ: (on average $x\%$ of columns)}, when CALIOP happens to hit a sufficiently thin cloud. To infer the cloud base height z at a point of interest (POI) that does not necessarily coincide with the location of a CALIOP profile, we proceed as follows. We first select all local CALIOP cloud base heights within a horizontal distance $D_{\max} = 100$ km of the POI that satisfy the additional quality cuts described in Section 3.2.

For each remaining local cloud base height z_i, we determine the predicted uncertainty σ_i based on the categories established in the previous section. We determine a combined cloud base height

$$z = \frac{\sum_i^n w_i z_i}{\sum_i^n w_i} \tag{3}$$

with weights

$$w_i = \frac{1}{\sigma_i^2} \qquad (4)$$

(optimal weights for uncorrelated least-squares). In practice, the individual measurements of cloud base are highly correlated with fairly similar σ_i. The cloud base estimate by Eq. (3) with weights given by Eq. (4) remains unbiased even in the presence of correlations. However, for the combined cloud base uncertainty, the uncorrelated weights would yield a biased estimate in the presence of correlations. The expression

$$\sigma^2 = \frac{1}{n} \sum_i^n \sigma_i^2 \qquad (5)$$

yields acceptable results, as would be expected for highly correlated and fairly similar σ_i. {j_μ: This i could be confused with the i in the previous section; rethink notation.}

One choice remains to be made, namely which of the bias correction methods described in Section 3.2 to apply to the local cloud base heights before combination. Combining the uncorrected local base heights result in a high bias (Figure S1), as would be expected from the high bias on the constituent local cloud base heights. The linear correction, which reduces the high bias for high cloud base heights but introduces a counterbias for low cloud base heights, leads to a low bias in the combined base height (Figure S2), again as would be expected. Among the correction methods investigated, the SVM-based correction results in the behavior closest to the 1-to-1 line (Figure S3). Based on this performance, we use the SVM-corrected local base heights as input to combination step of the CBASE algorithm.

3.4 Evaluation of cloud base heights and cloud base height errors

Having tuned the algorithm on data from the year 2008, we evaluate it using a statistically independent data set from the year 2007. In the evaluation data set, the "true" (i.e., measured by the ceilometer) cloud base height $\hat{z}$ is known in addition to the estimated cloud base height z and the estimated cloud base height uncertainty σ, determined according to the procedure described in the previous section. Figure 3 shows the joint distribution of CBASE and ceilometer-observed cloud base heights. (The difference between this figure and Figure S3 is that the underlying data is the validation, rather than the tuning, data set.)

For satellite-derived measurements of the cloud base height z that are unbiased with respect to the ceilometer-observed cloud base heights $\hat{z}$ and have correctly estimated uncertainties σ, the pdf of the quantity $(z - \hat{z})/\sigma$ has zero mean and unit standard deviation. In our evaluation data set, we find a mean of 0.04 and a standard deviation of 1.06, shown in Figure 4; this corresponds to a cloud base height bias of 4% and uncertainty bias of 6%, both relative to the predicted uncertainty. Thus, we find that both the cloud base estimate and the uncertainty estimate are unbiased at the better than 10% level.

7

As a further test of the reliability of the expected uncertainty, we divide the validation data set into deciles of the expected uncertainty. Table 2 shows that the actual RMSE within each decile is within 10% of the expected uncertainty and that linear regressions within each decile are close to the one-to-one line.

It is possible that cloud base height estimates outside North America could have greater biases or that greater uncertainty than this evaluation leads us to believe. This would be the case if continental clouds over North America are not representative of clouds elsewhere in a way that is not accounted for by the cloud properties taken into account by the uncertainty estimate. Since the validation sample spans an entire year on a continental scale, we expect that most cloud morphologies are included. However, certain cloud types exist that occur predominantly over ocean and present a particular challenge to the method, namely marine stratocumulus with horizontally extensive but vertically thin liquid-phase anvils. Due to the typical cloud base height uncertainty of several hundred m, the method is unlikely to be applied to stratocumulus cloud; nevertheless, a marine-cloud validation data set would be desirable. For the present work, no suitable marine-cloud evaluation data set was available; ship-based cloud base height observations were either based on human observers (unknown quality) or available only over a limited duration at limited locations, resulting in a severely statistics-limited set of coincidences with the CALIOP track.

{j_μ: Add a plot or table on layer geometry}

4 Results and data product availability

Geographic distributions of mean and median cloud base and thickness are shown in Figure 8 {j_μ: (which will be made from the CBASE data set when it's ready)}.

Comparison with 2B-GEOPROF-LIDAR cloud bases is shown in Figure 5. 2B-GEOPROF-LIDAR distinguishes between radar-only, lidar-only, and radar–lidar combined cloud bases; the latter category is rare for warm cloud and is not shown. For radar-only clouds, the mean error is large because the radar cloud base height predominantly clusters around the top of the ground clutter region with little dependence on the actual cloud base height. Lidar-only 2B-GEOPROF-LIDAR cloud base performs comparably to the CBASE cloud base on average; this is to be expected, as the underlying physical measurement is the same. Unlike 2B-GEOPROF-LIDAR, CBASE provides a validated uncertainty estimate, which allows an analysis using the cloud base heights to select only low-uncertainty cases or to statistically weight cloud base heights according to their uncertainty, as appropriate for the application.

Data {j_μ: for 2007 and 2008; do the other years later, perhaps with funding for the subadiabaticity study from somewhere} is available at DKRZ. {j_μ: Obtain DOI, put it here.}

Table 1. Statistics of the relationship between ceilometer and CALIOP cloud base height faceted by CALIOP VFM QA flag. Shown are the number of CALIOP profiles *n*, the product-moment correlation coefficient *r* between CALIOP and ceilometer cloud base heights, the RMSE, bias, and linear least-squares fit parameters.

```
## Error in mutate_impl(.data, dots): Evaluation error: object 'group1'
                                 not found.
```

5 Conclusions

We have presented the CBASE algorithm, which derives cloud base heights from CALIOP lidar profiles. This algorithm produces cloud base heights not only for thin clouds but also for clouds thick enough to attenuate the lidar (optical thickness $\tau \gtrsim 5$), based on the assumed homogeneity of cloud base height within an airmass. In addition to the cloud base height estimate, the CBASE algorithm supplies an expected uncertainty on the cloud base height. The CBASE data is available for the years 2007 and 2008 at $\{j_\mu$: insert DOI$\}$.

CBASE cloud base height and its uncertainty have been evaluated using ground-based airport ceilometer data over the contiguous United States, using a data sample unbiased by the tuning of the algorithm. The evaluation showed that cloud base height and cloud base height uncertainty is unbiased at the better than 10% level: the bias on the cloud base height is 4%, and the bias on the uncertainty is 6%, both relative to the expected uncertainty.

The performance of CBASE cloud base heights is similar to that of 2B-GEOPROF-LIDAR lidar-only cloud base heights, which are based on the same underlying physical measurement. However, the validated cloud base height uncertainty provided by CBASE allows for selection of only accurate cloud base heights or for statistically weighting of cloud base heights according to their expected uncertainty. This, in turn, makes the CBASE cloud base heights useful for pressing problems in climate research that require accurate knowledge of cloud geometry, such as cloud subadiabaticity, which will be presented in future work.
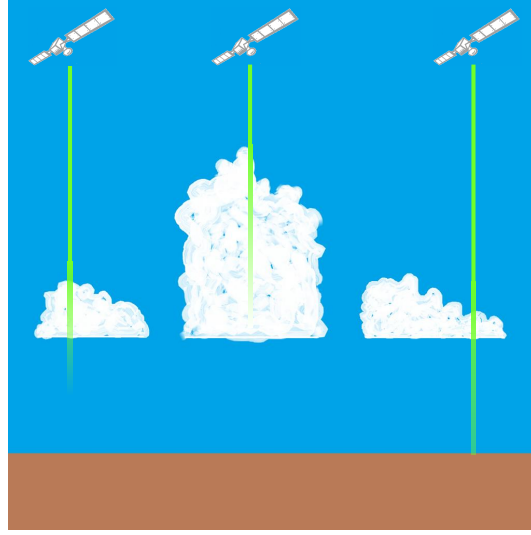
Figure 1. Schematic of CALIOP cloud base determination and evaluation strategy. In optically thick clouds, the lidar attenuates before reaching the cloud base, but the cloud base height of thin clouds can be used as a proxy for thick clouds in a cloud field with homogeneous cloud base height.

Figure 2. Scatter plots of CALIOP versus ceilometer local cloud base height faceted by the CALIOP VFM QA flag. Color indicates the number of CALIOP profiles within each bin of ceilometer and CALIOP cloud base height; black lines are contours of the empirical joint probability density; the red line is a linear least-squares fit, with 95% confidence interval shaded in light red; the blue line is a generalized additive model regression (**??**), with 95% confidence interval shaded in light blue; the dashed gray line is the one-to-one line. Statistics of the relationship between CALIOP and ceilometer base heights are provided in Table 1.

Table 2. CBASE cloud base statistics by decile of predicted uncertainty; see Table 1 for a description of the statistics provided.

| pred.rmse	n	r	RMSE (m)	bias (m)	fit
(167,427]	2624	0.741	404.	-46.9	$y = 1.03x + 28.0$ m
(427,453]	2624	0.719	429.	-28.4	$y = 1.06x - 32.0$ m
(453,469]	2624	0.703	461.	-18.8	$y = 1.09x - 87.7$ m
(469,484]	2624	0.685	463.	-17.8	$y = 1.03x - 18.3$ m
(484,497]	2624	0.628	506.	-6.06	$y = 0.976x + 33.4$ m
(497,508]	2624	0.574	547.	-8.73	$y = 0.986x + 25.5$ m
(508,522]	2624	0.596	547.	-14.1	$y = 1.01x + 5.37$ m
(522,541]	2624	0.572	562.	-9.26	$y = 0.967x + 49.6$ m
(541,573]	2624	0.502	639.	-22.7	$y = 0.939x + 96.8$ m
(573,748]	2624	0.447	720.	7.36	$y = 0.829x + 197.$ m
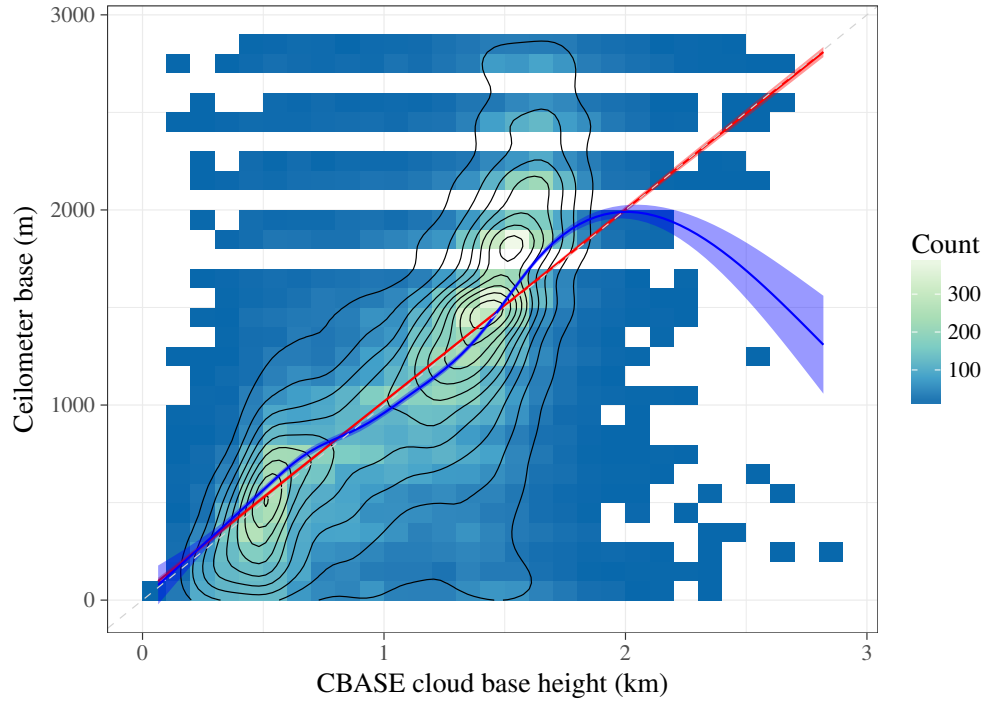
Figure 3. Scatter plot of CBASE versus ceilometer cloud base height; for description of the plot elements, see Figure 2. The linear fit has slope 0.98 and intercept 33.96 m.
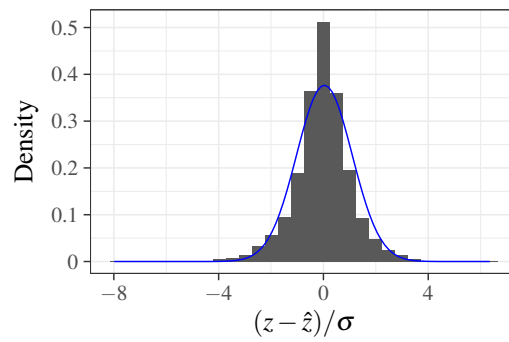

Figure 4. Distribution function of cloud base error divided by predicted uncertainty; for the ideal case of unbiased cloud base heights and unbiased uncertainty, the distribution would be gaussian with zero mean and unit standard deviation. The superimposed least-squares gaussian fit (blue line) has mean 0.04 and standard deviation 1.06.
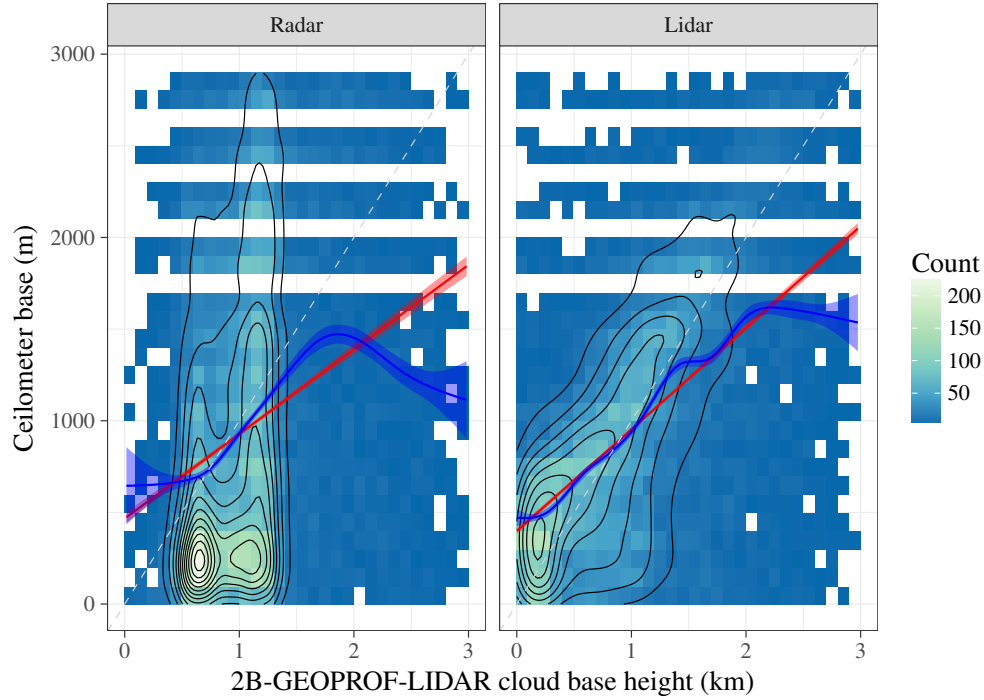
Figure 5. Scatter plot of 2B-GEOPROF-LIDAR versus ceilometer cloud base height faceted by the source of the cloud base (radar-only or lidar-only; due to their rare occurrence, combined radar–lidar base heights are not shown). For description of the plot elements, see Figure 2. Statistics of the relationship between 2B-GEOPROF-LIDAR and ceilometer base heights are provided in Table 3. {j_μ: I *think* this uses Claudia's algorithm (minimum cloud base within D_{max}), but I have to check.}

Table 3. Statistics of the relationship between ceilometer and 2B-GEOPROF-LIDAR cloud base height; see Table 1 for a description of the statistics provided.

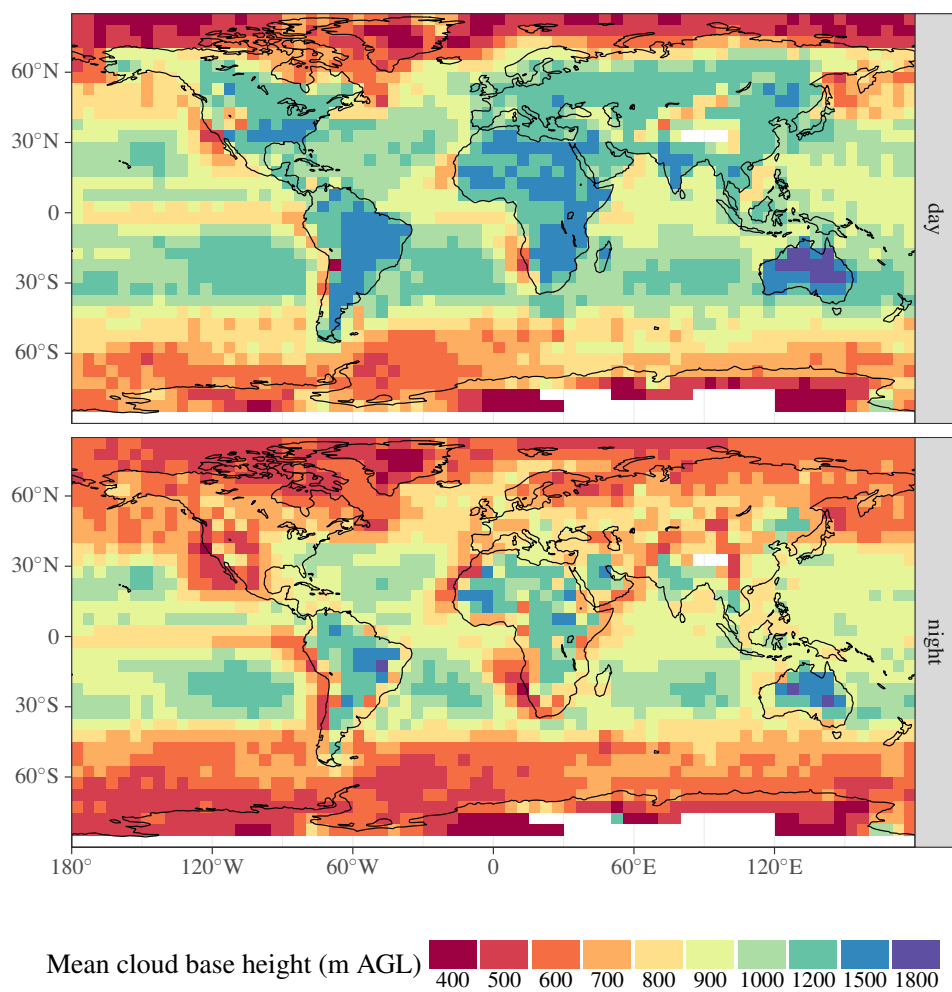| flag.base	n	r	RMSE (m)	bias (m)	fit
Radar	15061	0.265	782.	98.1	$y = 0.461x + 466.$ m
Lidar	12813	0.564	594.	16.3	$y = 0.555x + 399.$ m

Figure 6. Geographic distribution of mean cloud base heights above ground level. Statistics are calculated within each $5° × 5°$ latitude–longitude box, and separately for CALIOP daytime and nighttime overpasses.
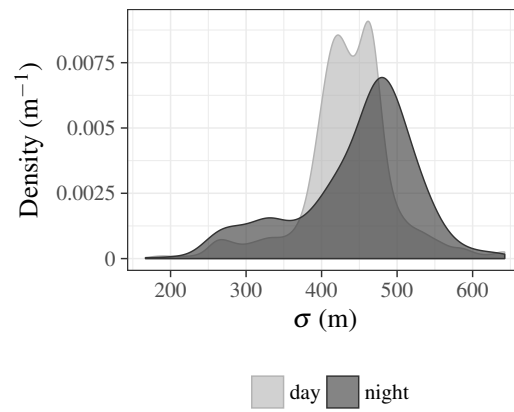
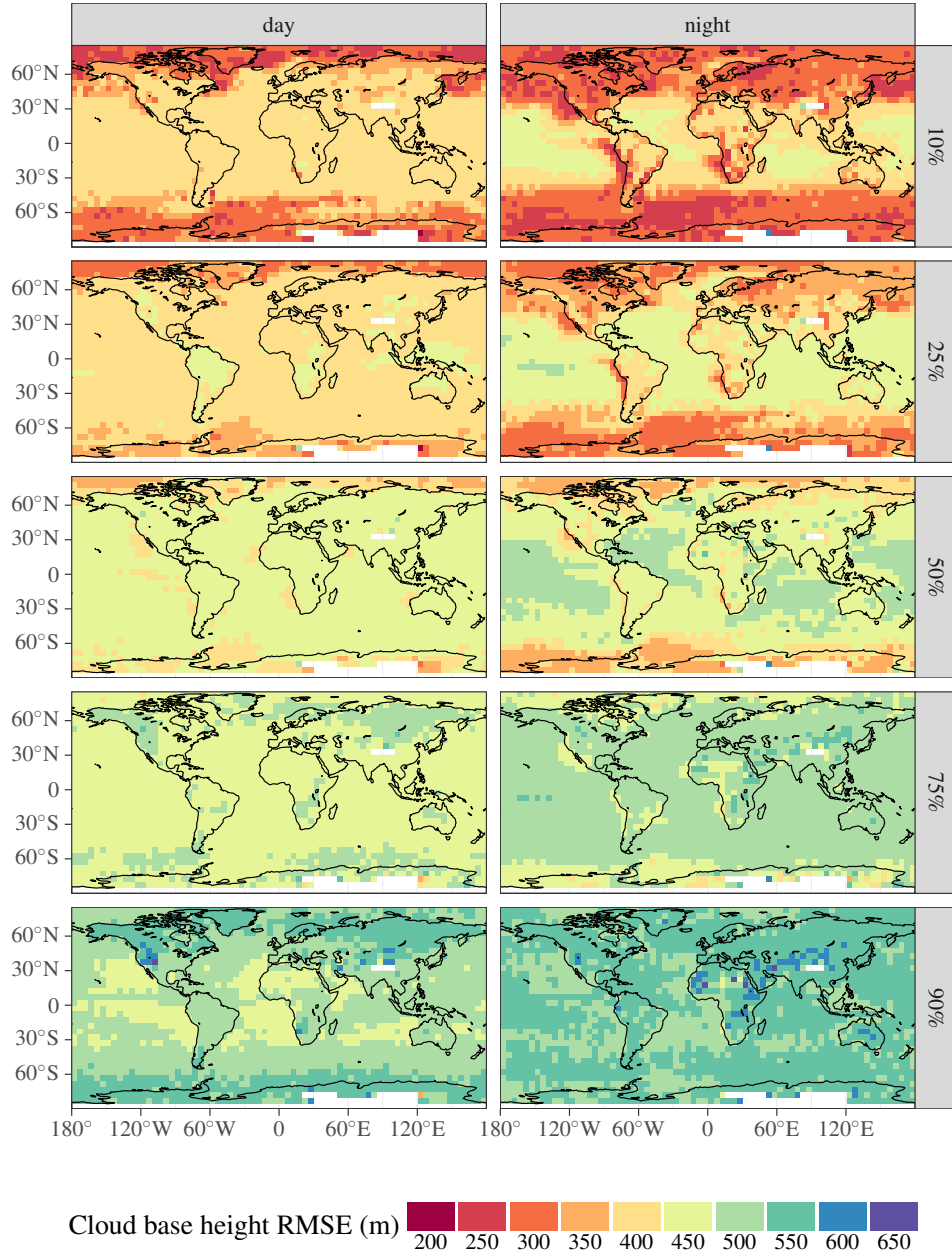**Figure 7.** Distribution of predicted cloud base height uncertainty.

Figure 8. Cloud base uncertainty quantiles. Statistics are calculated within each 5° × 5° latitude–longitude box. The left (right) column shows statistics of daytime (nighttime) retrievals; daytime and nighttime are defined by the CALIOP VFM product.